RELAXATION OSCILLATION SQUIDS WITH HIGH $\delta V/\delta\Phi$

D.J. Adelerhof, H. Nijstad, J. Flokstra, and H. Rogalla.
University of Twente, Department of Applied Physics, Low Temperature Group,
P.O. Box 217, 7500 AE Enschede, The Netherlands.

Abstract--Relaxation Oscillation SQUIDs (ROSs) based on Nb/Al,AlO_x/Al/Nb Josephson tunnel junctions have been designed and fabricated. The hysteretic SQUIDs have a maximum critical current of about 130 μA and an inductance of 20 pH. A voltage modulation of 400 μV and a flux to voltage transfer $\delta V/\delta\Phi$ of 4 mV/Φ_o have been measured in these SQUIDs. Double Relaxation Oscillation SQUIDs (DROSs), which are based on two hysteretic SQUIDs, showed transfer coefficients up to 77 mV/Φ_o. The intrinsic white flux noise of the DROSs is smaller than 3-5 $\mu\Phi_o/\sqrt{Hz}$. The results are very promising for a next generation of SQUID systems with simplified read-out.

I. INTRODUCTION

Present DC SQUIDs based on non-hysteretic shunted tunnel junctions [1] suffer from a relatively low flux-voltage transfer $\delta V/\delta\Phi$, which is typically of the order of 100 μV/Φ_o. Impedance matching at 4.2 K and ac flux modulation are necessary to reduce the deterioration of the sensitivity of the SQUID system by the input noise of the room temperature electronics. Sophisticated electronics is needed for read-out of the SQUID signal [2].

A Relaxation Oscillation SQUID (ROS) based on unshunted tunnel junctions offers the possibility to reduce the complexity of the read-out electronics, because large flux to voltage transfer coefficients can be achieved [3,4]. We have fabricated integrated ROSs based on Nb/AlO_x tunnel junctions. By numerical simulations the minimum and maximum values of the shunt inductance of the ROS have been calculated at different values of the shunt resistance. We aimed at the fabrication of ROSs with a sufficiently large SQUID inductance and a flux to voltage transfer of at least 1 mV/Φ_o. In SQUID systems based on such a ROS a matching transformer and flux modulation would not be necessary.

We also present the results on a Double Relaxation Oscillation SQUID (DROS) based on two hysteretic SQUIDs. The maximum flux to voltage transfer of DROSs is expected to be more than one order of magnitude larger than the maximum transfer of ROSs.

These investigations in the program of the Foundation for Fundamental Research on Matter (FOM) have been supported (in part) by the Netherlands Technology Foundation (STW).

II. THEORY

A schematic overview of a ROS is shown in fig. 1. A hysteretic SQUID with a maximum critical current $2I_o$ is shunted by an inductor L and a resistor R. If the bias current I_b is larger than the critical current $I_c(\Phi)$, relaxation oscillations can occur if RI_b is smaller than the gap voltage V_g of the junctions [5]. The voltage V across the SQUID will switch between 0 V and V_g. During time

$$t_0 = L/R \ln\left(\frac{I_b}{I_b - I_c}\right) \quad (1)$$

the voltage will be zero. The voltage will be equal to the gap voltage during

$$t_V = L/R \ln\left(\frac{I_c R}{V_g - I_b R} + 1\right) \quad (2)$$

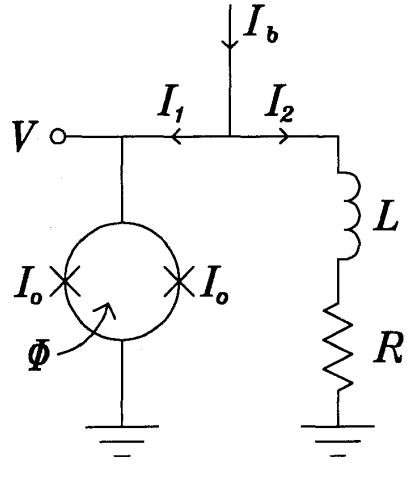

fig. 1 Schematic overview of a ROS.

Manuscript received August 24, 1992

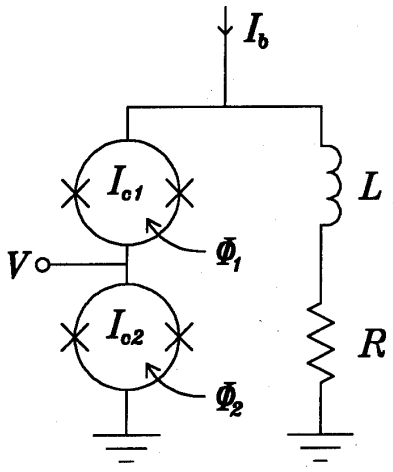

fig. 2 Schematic overview of a DROS

if the SQUID capacitance C_{SQ} can be neglected during the transition from V_g to 0 V. At a finite SQUID capacitance, however, the voltage state of the oscillations will be extended by a transition time t_c. This transition time is of the order of $C_{SQ}R_{sg}$, where R_{sg} is the subgap resistance of the SQUID. So, the average voltage across the SQUID is

$$\bar{V} = V_g \cdot \frac{t_V + t_c}{t_0 + t_V + t_c}. \qquad (3)$$

In fig. 2 a DROS is shown schematically. Two hysteretic SQUIDs in series are shunted by a resistor and an inductor. Φ_1 is the signal flux. The critical current I_{c2} can be adjusted by Φ_2. In this design Φ_1 and Φ_2 can be applied independently, which is different from the balanced ROS presented in ref. 3. If $I_{c1}<I_{c2}$, voltage V will be zero. If $I_{c1}>I_{c2}$, V will have a finite average value V_c. The maximum transfer coefficient at $I_{c1} = I_{c2}$ will be

$$\delta V/\delta\Phi_{max} = V_o/(\int^B \Phi_n^2(f)\cdot df)^{1/2}, \qquad (4)$$

where $\Phi_n(f)$ is the flux noise spectral density of the SQUID and B is the bandwidth.

III. OPERATION RANGE

In a ROS the relaxation oscillations can stop if $V = I_2 \cdot R = V_o$. The ROS can be locked to this stable situation during switching from V_g to 0 V, which is therefore the critical phase of the oscillations. In ref. 6 it is shown that a tunnel junction will switch back to the zero-voltage state if the (dc) bias current is decreased below a minimum value I_m. So, if the shunt resistance and the bias current are small enough to fulfill the condition $I_1(V_o) < 2I_m$, the ROS will always switch to the zero-voltage state, independent of the shunt inductance and the relaxation oscillations will not stop. The voltage output of such a ROS would be comparable to standard DC SQUIDs.

Since we aim at much higher flux-voltage transfers, we are interested in ROSs with $I_1(V_o) > 2I_m$. In this case, relaxation oscillations can only occur if the shunt inductance is within specific minimum and maximum values. The relaxation oscillations of a ROS have been simulated numerically in order to determine this operation range. The tunnel junctions are described by the RSJ model with a non-lineair quasi particle resistance. The junction specific capacitance is 0.03 pF/μm^2 [7].

The simulations showed that the operation range with respect to L becomes larger if the critical current density of the junctions increases. This is related to the increase of I_m at higher current densities [6]. The operation range of L decreases with increasing shunt resistance R. The optimum value of L/R is about $20C_{sq}R_{sg}(2\text{ mV})$, where $R_{sg}(2\text{ mV})$ is the subgap resistance of the SQUID at 2 mV. The ROS simulations will be presented elsewhere.

Based on these simulations we decided to fabricate ROSs and DROSs with $2I_o$ = 100 μA, $\beta_L = 2I_oL_s/\Phi_o = 1$, where L_s is the SQUID inductance, and a junction area of 16 μm^2. In the design of the SQUIDs 4 different values of L/R are incorporated: 5, 12, 19, and 26 ns. R is varied between 2.5 and 8.75 Ω. Consequently, the expected voltage modulation of the ROSs varies between 100 and 360 μV at I_b = 110 μA.

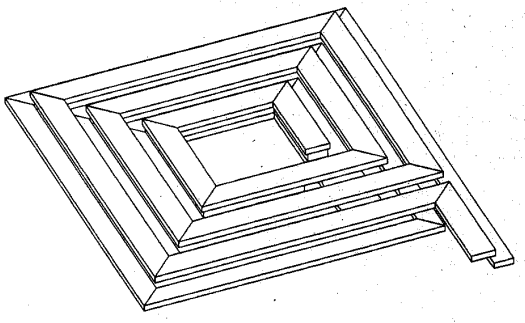

fig. 3 Two level multi-turn coil, with small parasitic capacitance

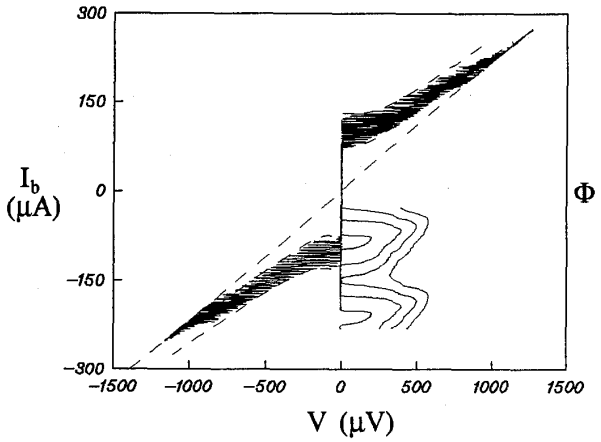

fig. 4 I-V characteristic and Φ-V curves of a flux modulated ROS. The dashed lines are theoretical I-V curves.

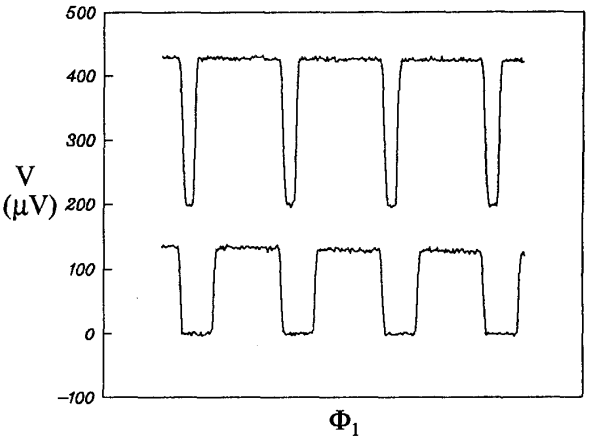

fig. 5 Φ-V characteristic of a DROS (R = 3.8 Ω, L = 46 nH) with constant bias current at two different values of Φ_2. The upper curve is shifted 200 μV upwards for clarity.

IV. FABRICATION PROCESS

The deposition of the Nb/Al,AlO_x/Al/Nb (SNINS) multilayer has been described in ref. 8. Junction areas have been defined by selective Nb etching in an RF SF_6 plasma. SiO_2 films, deposited by RF sputtering in an Ar/O_2 atmosphere, are used as insulator between the superconducting layers. By this process junctions with typical V_m values of 60-70 mV at 4.2 K can be made. (V_m = 2 mV·I_{th}/I(2 mV), where $I_{th} = \pi/4 \cdot V_g/R_n$ and R_n is the normal resistance of the junction at 4 mV.) The resistors were made of RF sputtered Pd [7].

The hysteretic SQUIDs are of square washer type, with a single turn input coil on top [9]. The shunt inductors consist of two stacked multi-turn coils as shown in fig. 3. The coils are separated by 350 nm of SiO_2, except for their central turns, which are in contact. The line width of the turns is 5 μm, the overlap between the turns is about 0.5 μm. The inductance of the coils is expected to be $L = 1.25n^2\mu_o d$, where d is the width of the central hole and n is the total number of turns [9]. In this way planar inductors with small parasitic capacitance can be made. The inductors are located at maximum distance from the SQUIDs (1-1.2 mm) to minimize the magnetic coupling with the SQUID.

V. ROS CHARACTERISTICS

Battery powered electronics was used to measure the characteristics of the SQUIDs. The input noise of the amplifier is 5 nV/√Hz.

The leads connecting the electronics to the SQUID are low-pass filtered at 1 MHz. The SQUIDs are partly shielded by a cryoperm and a lead pot.

In fig. 4 the I-V and Φ-V characteristics of a magnetic flux modulated ROS are shown. The shunt inductance of this ROS is designed to be 128 nH. This ROS shows modulation up to a bias current of about 220 μA. At higher bias currents the relaxation oscillations stop and $V = V_o$ = constant. At $I_b > 2I_o$ a voltage modulation of 400 μV can be obtained with a maximum slope $\delta V/\delta\Phi$ of 4 mV/Φ_o. Due to a small coupling between I_2 and the SQUID, the flux at which the maximum voltage is obtained shifts with changing bias current. The asymmetric Φ-V curves can be explained by this coupling as well.

The dashed lines in fig. 4 are theoretical curves describing the non-oscillating state with $V = V_o$, and the oscillating state with minimum and maximum critical current (eq. 1-3). The parameters obtained from the theoretical fit are $I_{c,max}$ = 130 μA, $I_{c,min}$ = 74 μA, R = 4.7 Ω, V_g = 2.75 mV, and $t_c = 0.03 \cdot L/R$. These values agree very well with the expected values except for the maximum critical current which is higher than intended.

In ROSs with a higher shunt resistance the maximum bias current at which the voltage is flux modulated is smaller than $2I_o$. Apparently, the oscillating state of these SQUIDs is less stable than the constant voltage state.

VI. DROS CHARACTERISTICS

Typical Φ-V characteristics of a DROS are

shown in fig. 5. The output voltage is almost a block function of Φ_1, as expected. The amplitude V_c of the modulation can be adjusted by the flux Φ_2 and the bias current. The maximum transfer coefficient $\delta V/\delta\Phi$ is obtained at $V \approx 0.5V_c$.

The SQUIDs used in the DROSs are identical to the SQUIDs used in the ROSs. DROSs with a shunt resistance smaller than 4-5 Ω all showed Φ-V characteristics similar to the curves depicted in fig. 5. The maximum value of $\delta V/\delta\Phi$ in these DROSs ranged from 20 up to 77 mV/Φ_o.

In several DROSs we measured the voltage noise with the DROS biased at the maximum flux-voltage transfer. At these bias points the contribution of the input voltage noise of the amplifier to the SQUID noise is negligible. From the voltage noise and $\delta V/\delta\Phi$ the flux noise has been calculated. In all cases the measured flux noise density is 3-5 $\mu\Phi_o/\sqrt{Hz}$ at 1 kHz. The noise gradually increases to 7-10 $\mu\Phi_o/\sqrt{Hz}$ at 1 Hz, without showing a clear 1/f behaviour. The similar flux noise characteristics of the DROSs strongly suggests that this noise level is determined by environmental noise. The measured maximum transfer coefficients $\delta V/\delta\Phi$ and the flux noise density are in agreement with eq. 4, if the bandwidth is taken to be 1 MHz, the cut-off frequency of the low-pass filters of our insert. Apparently, even steeper slopes $\delta V/\delta\Phi$ will be measured in a less noisy environment.

VII. CONCLUSIONS

We have fabricated relaxation oscillation SQUIDs based on Nb/AlO_x tunnel junctions with an inductance of 20 pH, a voltage modulation up to 400 μV, and a maximum transfer coefficient of 4 mV/Φ_o. The I-V characteristics of these SQUIDs can be well described by theory.

In double relaxation oscillation SQUIDs, $\delta V/\delta\Phi$ values up to 77 mV/Φ_o have been measured. The maximum Φ-V transfer is limited by the flux noise sensed by the SQUID. The intrinsic white flux noise level of these SQUIDs is smaller than 3-5 $\mu\Phi_o/\sqrt{Hz}$.

These results are very promising for the construction of SQUID systems with simplified read-out electronics.

REFERENCES

[1] C.D. Tesche and J. Clarke, *"dc SQUID: Noise and Optimization"*, J. Low Temp. Phys. vol 29, pp. 301-331, 1977.

[2] D. Drung, *"DC SQUID systems overview"*, Superc. Sci. Techn. vol. 4, pp. 377-385, (1991).

[3] S.A. Gudoshnikov, Yu.V. Maslennikov, V.K. Semenov, O.V. Snigirev, and A.V. Vasiliev, *"Relaxation Osillation Driven DC SQUIDs"*, IEEE Trans. Mag. vol. 25, pp. 1178-1181, 1989.

[4] Yu.V. Maslennikov, O.V. Snigirev, and A.V. Vasiliev, *"Integrated Relaxation Oscillation Driven DC SQUIDs"*, ISEC'87, Tokyo, pp. 144-146, 1987.

[5] F.L. Vernon and R.J. Pedersen, *"Relaxation Oscillations in Josephson Junctions"*, J. Appl. Phys. vol. 39, pp 2661-2664, 1968.

[6] H. H. Zappe, *"Minimum current and related topics in Josephson tunnel junction devices"*, J. Appl. Phys. vol. 44, pp 1371-1377, 1973.

[7] E.P. Houwman, *" Development of DC-SQUID sensors for multichannel magnetometry"*, PhD thesis, University of Twente, 1990.

[8] D.J. Adelerhof, E.P. Houwman, P.B.M. Fransen, D. Veldhuis, J. Flokstra, and H. Rogalla, *"Characterization of different types of Nb/AlO_x based Josephson tunnel junctions"*, IEEE Trans. Mag. vol. 27, pp. 3153-3156, 1991.

[9] J.M. Jaycox and M.B. Ketchen, *"Planar coupling scheme for ultra low noise DC SQUIDs"*, IEEE Trans. Mag. vol. 17 pp. 400-403, 1981.